

Segmentation of Masses Using Continuous Scale Representations

Andrew Laine^a, Walter Huda^b, Dongwei Chen^c and John Harris^c

^aDepartment of Computer and Information Sciences and Engineering, ^bDepartment of Radiology,

^cDepartment of Electrical and Computer Engineering
University of Florida, Gainesville, FL 32611. Email: laine@cis.ufl.edu

1. Introduction

Many image processing and computer vision algorithms are surprisingly fragile when it comes to choosing various parameters and thresholds. There have been no good solutions to setting the proper value of the scale parameter in regularization networks. Local adaptation is needed in these networks to make them less brittle. Using an assumption of zero-mean, additive Gaussian noise, it can be shown that the scale parameter for edge detection problems should be proportional to the variance of any additive noise [8]. However, these assumptions are too restrictive for most purposes, including digital mammography. More promising methods from Bayesian analysis are under investigation for setting the scale and other parameters by standard regularization-based methods [9]. The Laplacian filter is a popular edge detector in image processing [7]. However, knowledge of the feature size is necessary when choosing the proper scale for detection.

It is common to make some assumptions about feature characteristics. For example, we can assume that microcalcifications in mammograms occur within finer scales of analysis since these features are characterized by small, high-contrast spots. Unfortunately, it is more difficult to make such general assumptions for masses in mammograms since they may assume distinct shapes and sizes, e.g., spiculated, round, or irregular. Thus, it is necessary to identify an “optimal” scale for representation of masses. Once detected, their regions can be labeled to provide an area of local support for multiscale feature enhancement, including reinforcement of the “halo” effect, to assist in the visibility of masses [5, 6, 3].

In this paper, we describe a method to segment a mass from its background using a continuous multiscale analysis [2, 11, 10]. First, a suspicious region is identified, which may or may not contain a lesion. Next, the region is used as a matched filter to select a wavelet basis. A soft threshold is then applied. If the selected region contains a feature, the mammographic feature is segmented from its background for further processing.

2. Locating the Best Scale

In [4] we show how wavelet coefficients can be calculated at an arbitrary scale. Basis functions for carrying out continuous multiscale analysis were designed to be symmetric with zero-phase providing closed contours (via zero-crossings) of emergent features within each scale. We discuss a method for determining an appropriate scale for arbitrary mass

size within a local area. Using the image as a matched filter, a finite number of scales are searched within a local window to find the wavelet coefficients that most resemble a mass.

The method is demonstrated in Figure 1. The left-hand side of Figure 1(a) shows three scales of an image profile, containing bumps of distinct width. We calculated the wavelet transform for each image. At each scale, the maximum of wavelet coefficients across the shifting parameter was found. The relation between scale and the wavelet maximum is shown on the right-hand side of Figure 1(a). Note that there is exactly one scale a^* corresponding to the maximum of wavelet coefficients across both shifting and scale parameters. The value a^* is clearly a function of the size of the feature within the cropped region.

3. Application of the Segmentation Algorithm

X-ray images of an RMI model 156 phantom were investigated. The RMI phantom contains five masses and six fibrils which mimic two objects of interest in mammography. It is designed so that at least one object in each category is not visible and one object is at the borderline of the visibility threshold [1].

An X-ray image of the RMI phantom is ideal for studying image segmentation since it has well defined features of clinical interest which are present both above and below the threshold for visibility. Figure 2(a) shows a schematic representation of the insert in the phantom. Figure 2(b) shows an example of the corresponding radiographic image obtained with a conventional mammography unit.

The mass thickness/diameter characteristics for the masses were, for the borderline case (B) $500 \mu\text{m}/5\text{mm}$ and for the invisible case (I) $250 \mu\text{m}/3\text{mm}$. Digital radiographic images of the RMI phantom were obtained using a Digital Spot Mammography (DSM) system attached to a Lorad Breast Biopsy System (Lorad Corporation, Danbury, CT). The detector area was 50 mm by 50 mm which is smaller than the RMI phantom size shown in Figure 2. As a result, only 20 % was able to be captured in any single digital image. The DSM image matrix size used in this study was 512 by 512 so that the nominal pixel size was $100 \mu\text{m}$. For the mass region, technique factors of 22 kVp and 16 mAs were used. Additional images were also acquired at 32 kVp and 200 mAs, where the increased radiation reduced the noise and permitted the B/I masses to become visible. By this process, the locations of the invisible and borderline masses were established with a high level of accuracy. A 256 by 256 pixel region of interest incorporating the B mass was extracted for subsequent processing whereas for the invisible mass, a cropped region of 183 by 183, to eliminate extraneous objects.

Segmentation - Mass

Figure 3 shows representative images of the cropped regions corresponding to three masses (E, B and I). These images were generated using 22 kVp and 16 mAs. Also shown are the same four images after histogram equalization, unsharp masking, and window/leveling enhancement. The processed images in Figure 2 show negligible improvement in overall mass visibility using these traditional image enhancement techniques. Figure 4 shows the segmentation results obtained for a mass with borderline visibility. A profile through the center of mass and the corresponding profile of the wavelet coefficient is shown in Figure 4(c). Note that the interscale value $a = 28$ best defines the wavelet coefficient profile and

best segments the mass (Figure 4(b)). Figure 5 shows the segmentation results obtain for the invisible mass. A profile through the center of mass and the corresponding profile of the wavelet coefficients is shown in Figure 5(c). Here the interscale value $a = 28$ again best defines the wavelet coefficient profile and therefore best segments the mass (see Figure 5(b)). Thus the segmentation algorithm developed was capable of finding a mass which is normally invisible on standard radiographs of this phantom.

4. Summary

We have shown that regions corresponding to masses can be identified through frame representations of a continuous multiscale analysis. We showed that subtle features characteristic of mammographic findings required a finer parameterization of scale space than provided by traditional methods of wavelet analysis.

REFERENCES

- 1 A. G. Haus and M. J. Yaffe, editors. *A categorical course in physics: technical aspects of breast imaging*. 80th Scientific Assembly of the Radiological Society of North America (RSNA), Oak Brook, IL, 3rd edition, 1994.
- 2 I. Koren and A. Laine. A discrete dyadic wavelet transform for multidimensional feature analysis. In *Time-Frequency and Wavelets in Biomedical Engineering*. IEEE Press, 1997, to appear.
- 3 A. Laine, J. Fan, and W. Yang. Wavelets for contrast enhancement of digital mammography. *IEEE Engineering in Medicine and Biology Magazine*, 14(5):536–550, 1995.
- 4 A. F. Laine, W. Huda, D. Chen, and J. Harris. Local enhancement of masses using continuous scale representations. *Journal of Mathematical Imaging and Vision*, 7(1), 1997, to appear.
- 5 A. F. Laine, W. Huda, B. G. Steinbach, and J. C. Honeyman. Mammographic image processing using wavelet processing techniques. *European Radiology*, 5:518–523, 1995.
- 6 A. F. Laine, S. Schuler, J. Fan, and W. Huda. Mammographic feature enhancement by multiscale analysis. *IEEE Transactions on Medical Imaging*, 13(4):725–740, 1994.
- 7 D. Marr and E. C. Hildreth. Theory of edge detection. *Proceedings of the Royal Society of London*, 207:187–217, 1980.
- 8 J. L. Marroquin. Probabilistic solution of inverse problems. Technical Report, MIT Artificial Intelligence Laboratory, AI Memo No. 860, 1987.
- 9 R. Szeliski. *Bayesian modeling of uncertainty in low-level vision*. Kluwer Academic Publishers, Boston, MA, 1989.
- 10 M. Unser, A. Aldroubi, and S. J. Schiff. Fast implementation of the continuous wavelet transform with integer scales. *IEEE Transactions on Signal Processing*, 42(12):723–736, 1994.
- 11 A. Witkin. Scale space filtering. In *Proceedings of the International Joint Conference on Artificial Intelligence*, pages 1019–1022, Karlsruhe, Germany, 1983.

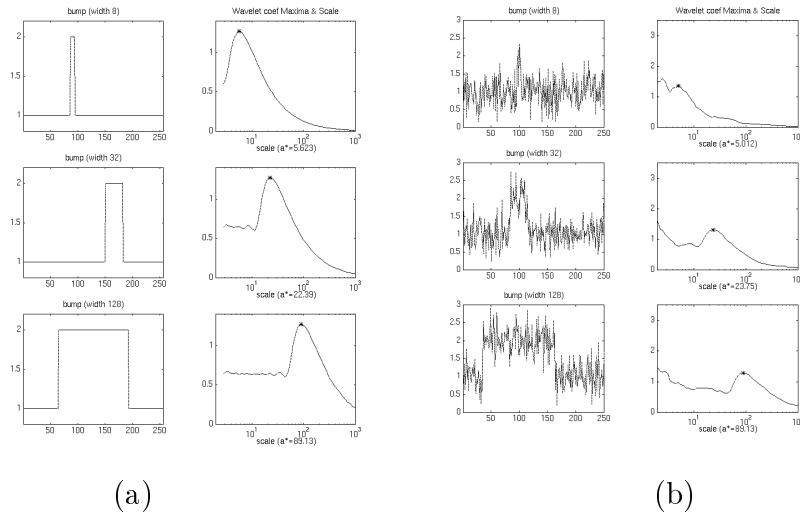


Figure 1. (a) The best scale to detect a bump in simulated mass profile of distinct size. (b) The best scale to detect a bump in noisy mass profiles.

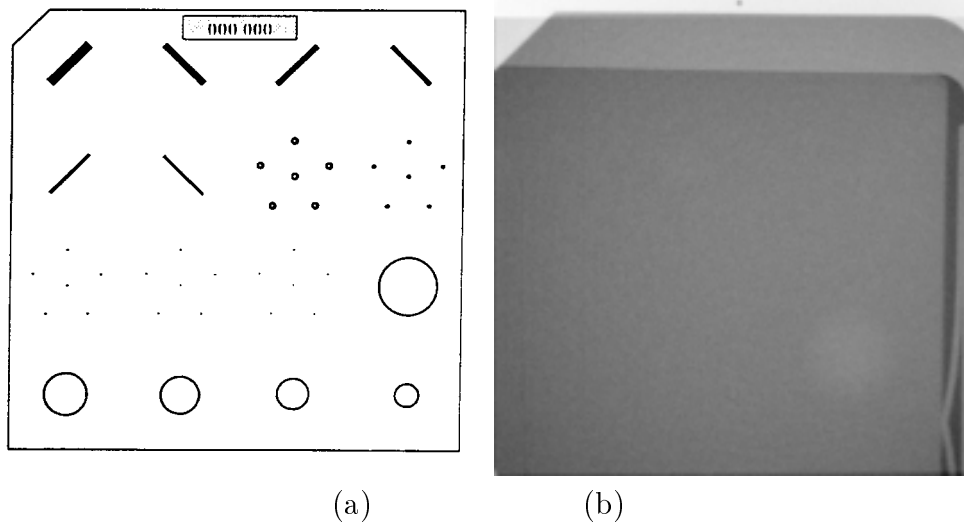


Figure 2. RMI phantom (Radiation Measurements Inc., Middleton, WI): (a) internal schematic; (b) digital radiograph.

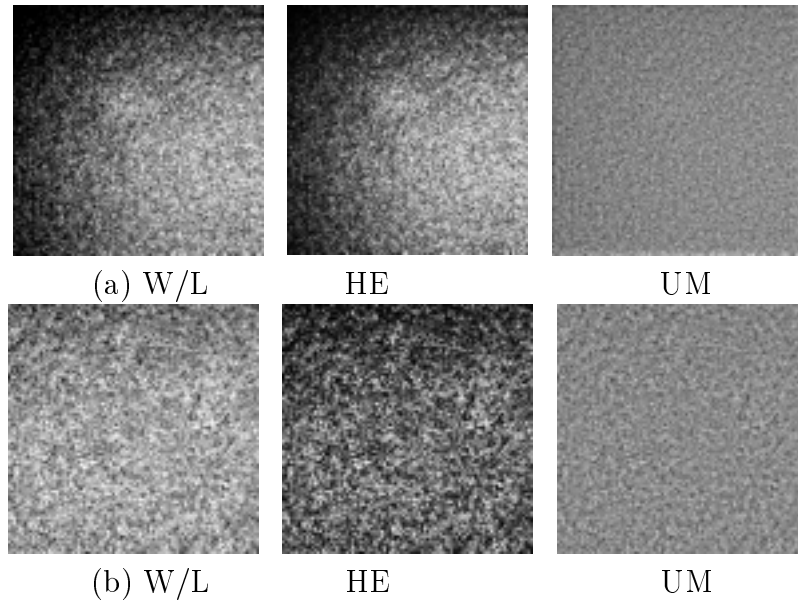


Figure 3. Traditional processing methods, window and leveling (W/L), histogram equalization (HE), unsharp masking (UM). (a) The borderline case; (b) the invisible case.

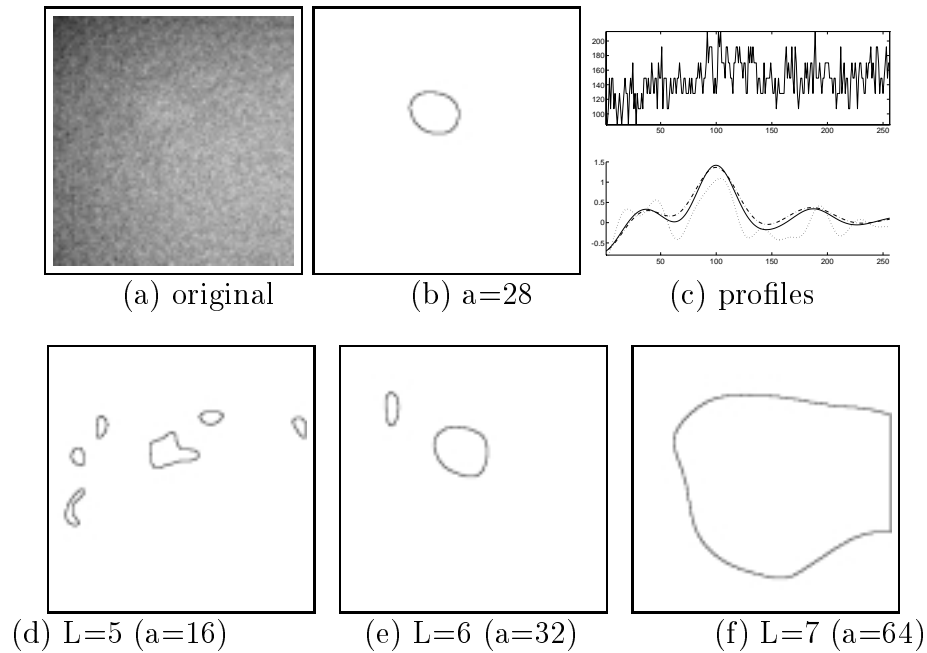


Figure 4. Mass (borderline) and multiscale edges: (a) original image (b) edges at best scale; (c) profile of mass (above) and wavelet coefficients (below) (d)–(f) dyadic scales.

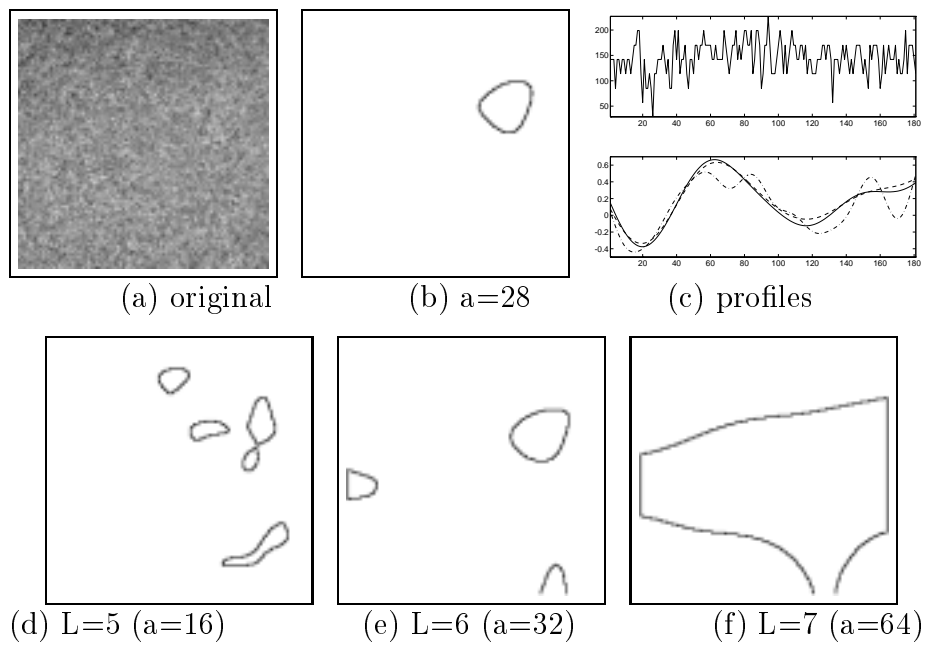


Figure 5. Mass (invisible) and multiscale edges: (a) original image; (b) edges at best scale; (c) profile of mass (above) and wavelet (below) coefficients; (d)–(f) dyadic scales